The Late Holocene to Pleistocene tephrostratigraphic record of Lake Ohrid (Albania)

Benoît Caron, Roberto Sulpizio, Giovanni Zanchetta, Giuseppe Siani, Roberto Santacroce

Elsevier Editorial System(tm) for Comptes rendus geoscience
Manuscript Draft

Manuscript Number:

Title: Tephrostratigraphie du Lac d'Ohrid (Albania) pendant le Pléistocène supérieure et l'Holocène. The Late Holocene to Pleistocene tephrostratigraphic record of Lake Ohrid (Albania).

Article Type: Full Length Article / Article original

Section/Category: - Géochronologie / Geochronology

Keywords: tephrostratigraphy; tephrochronology; Italian volcanoes; Lake Ohrid; Balkans; Albania

Corresponding Author: M. Benoit Caron, Ph.D. student

Corresponding Author's Institution: Università di Pisa

First Author: Benoit Caron, Ph.D. student

Order of Authors: Benoit Caron, Ph.D. student; Roberto Sulpizio; Giovanni Zanchetta; Giuseppe Siani; Roberto Santacroce

Abstract: Abstract
We present in this work a tephrostratigraphic record from a sediment piston core (JO-2004) from Lake Ohrid. Five tephra layers were recognised, all from explosive eruptions of south Italy volcanoes. A multidisciplinary study was carried out, including stratigraphy, AMS 14C chronology and geochemistry. The five tephra layers were correlated with terrestrial proximal counterparts and with both marine and lacustrine tephra layers already known in the central Mediterranean area. The oldest is from Pantelleria Island (P11, 131 ka BP). Other three tephra layers are from Campanian volcanoes: X6, Campanian Ignimbrite-Y5 and SMP1-Y3 (107, 39 and 31 ka BP respectively). The youngest tephra layer corresponds to the FL eruption from Etna Volcano (3.3 ka BP). In three cases these recognitions confirm previous findings in the Balkans, while two of them were for the

first time recognised in the area, with a significant enlargement of the previous assessed dispersal areas.

Résumé
Une étude tephrostratigraphique a été réalisée dans la carotte sédimentaire JO-2004 prélevée dans le Lac d'Ohrid. Cette étude bénéficie d'un cadre chronologique établi par sept datations SMA 14C et par des analyses chimiques des éléments majeurs. Cinq niveaux de tephra ont été détectés et corrélés aux dépôts terrestres proximaux ainsi qu'aux tephra identifiés dans des carottes marines et lacustres de la Méditerranée Centrale. Leur origine a été attribuée au volcanisme explosif du Sud de l'Italie et corrélée à l'activité de l'Ile de Pantelleria (P11, 131 ka BP), à la région Campanienne (X6, 107 ka; Ignimbrite Campanienne -Y5, 39 ka; SMP1-Y3; 31 ka) et à l'éruption FL de l'Etna (3,3 ka BP). Ces résultats sont en accord avec des travaux précédemment publiés dans la région des Balkans et ont permis d'identifier pour la première fois deux tephra (X6 et P11), en élargissant significativement leurs secteurs de dispersion en Méditerranéenne Centrale.

Suggested Reviewers: Maritne Paterne
Martine.Paterne@lsce.ipsl.fr

Sabine Wulf
swulf@ig.utexas.edu

Donatella Insinga
donatella.insinga@iamc.cnr.it

David Pyle
David.Pyle@earth.ox.ac.uk

Opposed Reviewers:

Tephrostratigraphie du Lac d'Ohrid (Albania) pendant le Pléistocène supérieure et l'Holocène

The Late Holocene to Pleistocene tephrostratigraphic record of Lake Ohrid (Albania).

Benoît Caron[1,3,*], Roberto Sulpizio[2], Giovanni Zanchetta[1], Giuseppe Siani[3], Roberto Santacroce[1]

[1] *Dipartimento di Scienze della Terra, via S. Maria 53, 56126, Pisa, Italy*

[2] *Dipartimento Geomineralogico and CIRISIVU, via Orabona 4, 70125, Bari, Italy*

[3] *IDES-UMR 8148, Département des Sciences de la Terre, Université Paris-XI, 91405 Orsay, France*

[*] Corresponding author: Benoît Caron, Dipartimento di Scienze della Terra, via S. Maria 53, 56126, Pisa, Italy, tel.: +39 050 22 15 700, fax: +39 050 22 15 800, caron@dst.unipi.it

Abstract

We present in this work a tephrostratigraphic record from a sediment piston core (JO-2004) from Lake Ohrid. Five tephra layers were recognised, all from explosive eruptions of south Italy volcanoes. A multidisciplinary study was carried out, including stratigraphy, AMS ^{14}C chronology and geochemistry. The five tephra layers were correlated with terrestrial proximal counterparts and with both marine and lacustrine tephra layers already known in the central Mediterranean area. The oldest is from Pantelleria Island (P11, 131 ka BP). Other three tephra layers are from Campanian volcanoes: X6, Campanian Ignimbrite-Y5 and SMP1-Y3 (107, 39 and 31 ka BP respectively). The youngest tephra layer corresponds to the FL eruption from Etna Volcano (3.3 ka BP). In three cases these recognitions confirm previous findings in the Balkans, while two of them were for the first time recognised in the area, with a significant enlargement of the previous assessed dispersal areas.

Résumé

Une étude tephrostratigraphique a été réalisée dans la carotte sédimentaire JO-2004 prélevée dans le Lac d'Ohrid. Cette étude bénéficie d'un cadre chronologique établi par sept datations SMA ^{14}C et par des analyses chimiques des éléments majeurs. Cinq niveaux de tephra ont été détectés et corrélés aux dépôts terrestres proximaux ainsi qu'aux tephra identifiés dans des carottes marines et lacustres de la Méditerranée Centrale. Leur origine a été attribuée au volcanisme explosif du Sud de l'Italie et corrélée à l'activité de l'Ile de Pantelleria (P11, 131 ka BP), à la région Campanienne (X6, 107 ka; Ignimbrite Campanienne -Y5, 39 ka; SMP1-Y3; 31 ka) et à l'éruption FL de l'Etna (3,3 ka BP). Ces résultats sont en accord avec des travaux précédemment publiés dans la région des Balkans et ont permis d'identifier pour la première fois deux tephra (X6 et P11), en élargissant significativement leurs secteurs de dispersion en Méditerranéenne Centrale.

Keywords: tephrostratigraphy, tephrochronology, Italian volcanoes, Lake Ohrid, Albania

1. Introduction:

Tephrostratigraphy is a powerful tool that is widely applied to volcanology, Quaternary science, palaeoceanography or archaeology. This is particularly true in the central Mediterranean region, which bore witness to frequent and powerful volcanic explosive activity during both Holocene and Late Pleistocene [5, 6, 7, 10, 18, 25, 28, 29, 31, 35, 36, 37, 39, 44, 47]. Some of the tephra layers generated during these explosive eruptions have regional or extra-regional relevance (e.g. Y3, Y5, Y6, Y7, X5 and X6 tephra layers) [8, 10, 20, 32, 39, 42, 49], since they covered very wide areas facilitating correlations between different geological archives. Many other tephra layers are less dispersed but are frequently recognised in marine and lacustrine cores drilled in the central Mediterranean area [4, 14, 16, 17, 28, 30, 40, 46, 47]. Owing to its position downwind of the Italian volcanoes, the Balkans were affected by tephra deposition during Holocene and late Pleistocene [41, 46] (Fig. 1), but tephrostratigraphic studies are few and limited to the last 40 ka. This paper deals with the study of a long core (JO 2004; 9.88 m), collected on the Albanian side of Lake Ohrid, which records the last 130-140 ka of sedimentation [13]. Our aim is to provide a tephrostratigraphic reconstruction of the core JO 2004, and to provide the correlation of its tephra layers with marine, lacustrine or terrestrial deposits in the central Mediterranean. The correlation among the different archives provides an updated framework of the tephra dispersion in the central Mediterranean area, and particularly in the Balkans.

Few tephra studies were carried out in the Balkans [41, 46], although their downwind position from the Italian volcanoes makes the area particularly subjected to distal ash deposition. On the other hand, the recognition of ash layers from Italian volcanoes in the Balkans contributes to shed light into the complex and poorly understood dynamics of dispersal of ash particles during and after explosive eruptions.

2. Site description

The Ohrid Lake is one of the oldest lake in Europe [38], and is located at the border between Albania and Macedonia (40°54'-41°10' N; 20°38'-20°48' E) (Fig. 1). The lake is at 705 m a.s.l., and has a surface of about 360 km². It is surrounded by two principals mountain chains: the Galiçica Mountains to the east (more than 1750 m a.s.l.), and the Mokra Mountains to the west (around 1500 m a.s.l.; Fig. 1). The Lake Ohrid has a NS orientation, and is located in a graben which formed during the extension of the Albanian area during the Pleistocene [1, 46]. Carbonate rocks of Triassic and Jurassic age crop out to the north and to the east, while ophiolitic rocks of Jurassic age crop out to the south-west. The southern end of the basin connects with a small graben filled by continental mudstones and sandstones of Pliocene age, overlain by fluvio-lacustrine sediments of Holocene age [24]. The Lake Prespa, located 20 km to the south-east and 150 m above the Lake Ohrid, is the principal sub-aquatic inflow of Lake Ohrid through a karstic system located below the Galiçica Mountain Chain. The Black Drin River is the only surface outflow to the north part of the Lake Ohrid [2, 21, 38].

3. Materials and methods.

Two series of piston cores (JO 2004-1 and JO 2004-1a) were drilled in the south west part of the Lake Orhid (40° 55,000' N ; 20° 40,297' E ; Fig. 1). The uppermost roughly 10 m of sediments were recovered using a cable-operated piston-core (63 mm in diameter and 3 m-long; Niederreiter Corer). In order to obtain a continuous sediment record, four sections (labelled A, B, C and D respectively from the top to the base) were cored from a first drilling site (JO 2004-1), and three sections (labelled A, B and C) with a planed depth offset of 1.5 m from a second drilling site located at about 5 m of distance from the first (JO 2004-1a; Fig. 2). The overlapping sections were correlated using marker layers clearly identified in both cores and the resulting composite profile checked for consistency using the magnetic susceptibility record (Fig. 2b).

The magnetic susceptibility of core JO 2004 has not permitted the identification of any tephra layer, due to the high noise induced by the magnetic minerals from the drainage basin bedrocks

[46]. Tephra layer were identified by continuously sampling the composite profile at 1 cm-interval, and washing and sieving each sample at 125, 63 and 40 μm using distilled water. The different grain size fractions were dried in a laboratory heater at a temperature of 50°C over 24 h. The three sediment fractions were carefully inspected under the stereo-microscope, looking for volcanic particles (i.e. glass shards, pumice, magmatic crystals, volcanic lithics). At least 400 particles were counted under the stereo-microscope to obtain the glass abundance.

In samples with volcanic glass in excess of 10 %, glass shards and micro-pumice fragments were picked and sealed in resin beads. They were then polished to avoid compositional variations caused by surface alteration processes.

Major element compositions of glass was obtained using an EDAX-DX micro-analyser (EDS analyses) mounted on a Philips SEM 515 at Dipartimento di Scienze della Terra (University of Pisa). Operating conditions were: 20 kV acceleration voltage, 100 s live counting, 10^{-9} Å beam current, beam diameter ≈500 μm, 2100 shots per second, ZAF correction. The ZAF correction procedure does not include natural or synthetic standards for reference, and requires the analyses normalization at a given value (which is chosen at 100%). Instrument calibration and performance are described in Marianelli and Sbrana [19].

The composition of glass was classified using the Total Alkali vs. Silica diagram (TAS, [12], Fig. 3a).

Seven ^{14}C radiocarbon datings were available from literature [13] (Table 3). Raw radiocarbon measurements were converted into calibrated ages using the INTCAL04 method [33] and the polynomial equation of Bard et al. [3] for ^{14}C ages older than 26 cal ka BP.

4. Results

Five tephra layers were recognised along the composite profile, and labelled JO-941 (938 – 942 cm), JO-575 (571 – 577 cm), JO-244 (235 – 252 cm), JO-187 (185.5 – 188.5 cm) and JO-42 (36.5 – 45.5 cm), respectively (Fig. 2a and b).

4.1. Cryptotephra JO-941 (938 – 942 cm)

The deepest tephra is dispersed in the sediment (cryptotephra), and glass shards were recognised in all the three sieving classes. The peak of abundance of glass particles is at 941 cm (60 %; Fig. 2c), and comprises transparent, brown-honey, cuspated, thin glass shards (Fig. 4a). The groundmass is glassy, and EDS analyses show a homogeneous rhyolitic composition (Fig. 3a and b, Table 1). In the diagram Comendite-Pantellerite (FeO vs. Al_2O_3; [15]) all the analysed samples plot into the pantelleritic field.

4.2. Cryptotephra JO-575 (571 – 577 cm)

This cryptotephra mainly comprises white to light-brown, elongated and cuspated glass shards and rare, white micro-pumice fragments (Fig. 4b). The peak abundance of glass shards is between 574 and 575 cm (95 %; Fig. 2c). The groundmass is glassy (Fig. 4b), and the composition shows a small variability within the trachy-phonolitic field (Fig. 3a and c; Table 1).

4.3. Tephra layer JO-244 (235 – 252 cm)

This tephra layer is composed of two distinct parts with different colours. The first one (between 244 and 244.5 cm) is Yellowish Gray (5Y 7/2; [9]), while the second one (between 247 and 248 cm) is Moderate Olive Brown (5Y 4/4; [9]). The tephra comprises white, vesicular micro-pumices and elongated glass shards with thin septa. Most of the glass shards are transparent, with few dark-brown in colour (Fig. 4c). The abundance of glass shards and micro-pumice has its maximum (100 %) between 244 and 244.5 cm (Fig. 2c). The groundmass is glassy (Fig.4c), and the glass composition is trachy-phonolitic (Fig. 3a and d; Table 1).

4.4. Tephra layer JO-187 (185.5 – 188.5 cm)

This tephra layer is Yellowish Gray in colour (5Y 4/1; [9]), and comprises transparent, tubular, elongated micro-pumice fragments and transparent, brownish glass shards (Fig. 4d). The

maximum abundance (99%) is at 187 cm (Fig. 2c). The groundmass is glassy (Fig. 4d), and the glass composition is homogeneous and trachytic (Fig. 3a and e; Table 1).

4.5. Cryptotephra JO-42 (36.5 – 45.5 cm)

This cryptotephra has a peak abundance of glass particles (80%) at 42 cm of depth (Fig. 2c), and comprises dark-brown, blocky, tachylitic fragments with few spherical vesicles (Fig. 4e). The groundmass comprises small crystals of plagioclase, clinopyroxene and minor olivine (Fig. 4e). The glass composition ranges between mugearites and benmoreites (Fig. 3a and f).

5. Discussion

5.1. Correlation of tephra layers

The K- to Na-alkaline affinity of glass compositions of the five tephra layers recognised in the core JO 2004 indicate that all of them were from explosive eruptions of Italian volcanoes, since during late Quaternary the products of the Aegean arc were characterised by calc-alkaline affinity [10, 30, 42]. Two of them (JO-941 and JO-42) present peculiar glass composition that indicate a source from Pantelleria Island and from Mount Etna, respectively. The other three tephras display trachytic to phonolitic composition, and can be correlated to the explosive activity of Campanian volcanoes. In the following, the precise correlation of each tephra layer with a specific eruption of these volcanoes will be discussed in detail. For comparison, the average compositions of the correlated tephra layers are reported in Table 2.

Cryptotephra JO-941

The pantelleritic glass composition of cryptotephra JO-941 (Table 1) indicates it was generated from Pantelleria Island. The Island of Pantelleria produced several large explosive eruptions with pantelleritic composition [18]. Among them, the most dispersed are the Green Tuff (45-50 ka BP), the Ignimbrite Q (113.9 ± 3.6 ka BP), the Ignimbrite P (133.1 ± 3.3 ka BP), the Welded

tuff S (162-164 ka BP) and the Welded tuff M (174.8 ± 2.8 ka BP; [18]). Two other $^{40}Ar/^{39}Ar$ datings are available for the Ignimbrite P (126.8 ± 1.5 ka BP) and for the Welded tuff S (174.5 ± 1.5 ka BP; La Felice, pers. com.). Pantelleritic tephra layers have been found in the Ionian Sea core KET 8222 [30] (Table 2) and named P11 (estimated age at about 131 ka BP, 555 cm depth) and P12 (estimated age at about 164 ka BP, 765 cm depth), which have similar ages of Ignimbrite P and Welded tuff S. The composition of P11 and P12 is quite similar, and the two tephra layers are hardly distinguishable on the basis of major elements.

The glass composition of sample JO-941 matches well that of both tephra layers P11 and P12 (Tables 1 and 2, Fig. 3b). Indeed, the tephra layer P11 have been recognised over a wide area of the Ionian sea while the dispersal of P12 is more limited [30]. Nevertheless, stratigraphic and paleoclimatic considerations support the correlation of the JO-941 cm tephra with P11 marine tephra layer, and then with Ignimbrite P deposits on Pantelleria Island. This is because both carbonate and pollen curves carried out on JO 2004 core sediments [13] inequivocally indicate that this tephra were emplaced close to the inception of the Last Interglacial. The onset of the Last Interglacial may have been recorded at different times in different archives [43], but, in any case, the age of 164 cal ka BP (which corresponds to P12 tephra layer) is too old of some ten thousand years with respect to that commonly accepted for the inception of Last Interglacial at Mediterranean latitudes (e.g. 126.8 and 120.3 ka BP ; [43]).

The recognition of tephra layer P11 is the first in the Balkans, and significantly enlarges its dispersal well beyond the Ionian sea (Fig. 5a).

Cryptotephra JO-575

This low alkali ratio (LAR) trachytic tephra layer occurs between the calibrated ^{14}C age of 44,812 ± 1055 cal yrs BP [13] (Table 3) and the P11 tephra layer.

Composition of the tephra layer JO-575 shows a good match with marine tephra C-31 (KET 8222 and DED 8708 deep sea cores, Fig. 3c and Table 2), which has an interpolated age of 107 ka BP [30]. Paterne had related the C-31 tephra with the LAR- trachyte X6 from 22M-60 core

[10]. So, the glass composition of JO-575 tephra layer is correlated to the X6 tephra layer. This X6 tephra layer is also dated at 107 ka BP by interpolation from $^{40}Ar/^{39}Ar$ age of the X5 tephra layer (105 ± 2 ka) by Kraml [11] using the sediment rate.

Keller in 1978 [10] attributed the X6 eruption to the Campanian volcanic zone.The X6 tephra layer was for the first time described in Ionian sea cores [10], and successively in Tyrrhenian sea core [30] as well in the Lago Grande di Monticchio succession [48]. This is the first recognition of X6 tephra layer in the Balkans, and considerably enlarges its dispersal area to the east (Fig. 5b).

Tephra layer JO-244

This tephra layer is 11 cm thick (Fig. 2) and comprises both glass shards and micro-pumice fragments. When plotted on TAS diagram (Fig. 3a) the glass composition has a narrow variability within the trachytic and phonolitic fields. However, the tephra layer shows a variable alkali ratio passing from the base to the top. In particular, the basal part shows the coexistence of glasses with two different alkali ratio (Table 1, Fig. 3d), whereas upper part has a very homogeneous LAR-trachytic glass composition (Table 1).

The glass composition indicates the Campanian area as source for this tephra that, on the basis of the peculiar variability in alkali ratio and the thickness, can be confidently correlated to the Campanian Ignimbrite eruption from Campi Flegrei. The geochemical comparison of major element shown in Table 2 is applied with the ML-2 layer [20] and the TM-18 layer [47] among the many analyses available. The Campanian Ignimbrite eruption was dated at 39,280 ± 110 yrs BP ($^{40}Ar/^{39}Ar$ technique; [6]), and correspond to the Y5 tephra layer, widely dispersed in the central and eastern Mediterranean and in mainland Europe [8, 10, 20, 23, 27, 28, 32, 39, 45, 46, 47]. The recognition in Lake Ohrid succession confirms the previous finding of Wagner et al. [46] (Fig. 5c).

Tephra layer JO-187

The JO-187 tephra is chronogically constrained between the Campanian Ignimbrite (≈ 39 ka BP) and the ^{14}C age of 9,407 ± 121 cal yrs BP obtained at 100 cm depth (Table 3). The homogeneous trachytic composition (Table 1, Fig. 2e) of this tephra layer suggests it was originated from the Campanian area, and shows a good match with the composition of SMP1-e eruption from Campi Flegrei [7]. The SMP1-e eruption corresponds to the Y3 tephra layer (Table 2 ; [7, 39, 49]), which is widely dispersed in the central Mediterranean area [10, 22, 23, 39, 47, 49] with an estimated age between 30 to 31 cal ka BP [49]. The recognition in Lake Ohrid succession confirms the previous finding of Wagner et al. (2008) [46] (Fig. 5d).

Cryptotephra JO-42

This cryptotephra is stratigraphically younger than the ^{14}C age of 6,680 ± 66 cal yrs BP (Table 3), and the peculiar mugearitic-benmoreitic composition easily indicates the Mount Etna as the source. The shallow position within the core and the glass composition indicates a correlation with the FL eruption from Mount Etna, dated at 3,370 ± 70 cal yr BP [5, 46]. The recognition in Lake Ohrid succession confirms the previous finding in the same lake (Macedonian side) of Wagner et al. [46] and of Sulpizio et al. [41] which recovered the Etna FL tephra layer in the Lake Shkodra successions (Albania) (Fig. 5e).

5.2. Significance of tephra layer recognition in Lake Ohrid

The recognition of tephra layers in the Lake Ohrid has relevance for both volcanology and Quaternary sciences.

From a volcanological point of view, the five tephra layers recognised in the sediments testify for episodes of ash deposition in very distal areas with respect to the Italian volcanoes (Fig. 5), irrespective if they are from large (P11, X6, Y5 and Y3 tephra layers) or intermediate (FL tephra layer) explosive eruptions.

Three out of five tephra layers were already recognised in Lake Ohrid sediments (Y5, Y3, and FL) but from a core located in the Macedonian side of the lake [46]. Their recognition in core

JO 2004, confirm their deposition was not sporadic but probably they affected all the lake area and its drainage basin. Two of them (P11 and X6) were recognised for the first time in the Balkan area, significantly enlarging to the North-East their dispersal that was previously limited to Ionian and Tyrrhenian seas [10, 30] or Lago Grande di Monticchio [48]. These new findings represent the most distal recovering of these two eruptions, that is more than 1,000 km from Pantelleria Island and more than 500 km from the Campanian area (Fig. 5).

The paucity of accurate studies on distal ash deposits mainly relies in their poor preservation and in their dispersal behaviour. The accumulation of volcanic ash in distal zones often represents a hazard, since most of the attention and mitigation procedures are usually devoted to proximal areas. Deposition of ash in distal sites can cause damage to infrastructures, disturbance to communications, water pollution and breathing problems. Therefore the recognition and the collection of very distal samples can improve hazard mitigation plans and procedures over very large area far from the volcanic sources.

Form a Quaternary science point of view, the lake Ohrid represents an exceptional natural archive. Previous works [46] analysed and discussed only the last 40 ka of sedimentation and paleoclimatic record of Lake Ohrid. The cores JO 2004 offer the opportunity to study about 130 ka of the sedimentary record, which encompass the last interglacial. In this scenario, the presence of two important regional markers like the P11 and X6 tephra layers allow the physical correlation of the deep part of the cores JO 2004 to other important archives of the central Mediterranean area.

The available ^{14}C datings (Table 3) and the tephra layers allow the drawing of a sedimentation curve (Fig. 6). The sediment curve based on the seven ^{14}C dating and on the tephrochronology, shows three main different rates of sedimentation. The first one between 0 and 100 cm of depth is about 0.10 mm yr^{-1}, the second one, between 100 and 575 cm of depth is around 0.05 mm yr^{-1} and the third one between 575 and 988 cm of depth is about 0.15 mm yr^{-1} (Fig. 6).

These variable sedimentation rates reflect different paleo-environmental information. Below the X6 tephra layer, there is the transition between the last-glacial and the last-interglacial

phases (Eemian, transition from marine isotopic stage 5 and 6, around 125 ka BP; [13]), which was characterised by a high sedimentation rate (0.15 mm yr^{-1}; Fig. 6). Between 100 and 575 cm depth, there is a glacial period record with a low sedimentation rate (0.05 mm yr^{-1}) and low sediment dynamic. The upper 100 cm of core sediments (younger than 10 ka BP), correspond to the current interglacial period, which is characterised by a high sedimentation rate (0.11 mm yr^{-1}).

6. Conclusions

The study of the JO 2004 cores yields some important results for the tephostratigraphy and tephrochronology of the Balkans. Five tephra layers were recognised and described, and two of them were for the first time discovered in the area. The tephra layer P11 is the oldest in the whole recognised succession and testifies for ash deposition at more than 1,000 km from its source on Pantelleria Island. Similarly, the recognition of tephra layer X6 enlarges to the east its dispersal, since it was previously described only in Ionian and Tyrrhenian Sea cores and in the Lago Grande di Monticchio. The other three tephra layers (FL, Y3 and Y5) were already recognised in Lake Ohrid succession, and the new findings testify for their extensive deposition in the area.

The recognition of the two deeper tephra layers (X6 and P11) is especially important, since they allow the establishment of a chronology for the part of the core older than 40 ka BP, and its physical link to other archives of the central Mediterranean area.

In perspective, this work will allow to obtain a better estimation of the distal tephra dispersion from Italian volcanoes. These results must be integrated in the mitigation and rescue plans which concern the population of Central Mediterranean area.

Acknowledgements:

We acknowledge the French (INSU-CNRS) research program ECLIPSE, the French School of Athens (Greece) and the Archaeological museum of Korça (Albania) for financial support and authorizations. We thank Anne-Marie Lézine, Uli von Grafenstein and Nils Andersen for providing samples for the piston core JO 2004 and for the useful discussions. Alain Mazaud is thanked for the magnetic susceptibility. BC was partially supported by Vinci program of Université Franco-Italienne and SETCI from region of Île-de-France. Franco Colarieti (DST Pisa) is gratefully acknowledged for the preparation of samples and assistance during EDS analyses. Amandine Bordon and Soumaya Belmecheri are thanked for helpful discussions.

References

[1] S. Aliaj, G. Baldassarre, D. Shkupi, Quaternari subsidence zones in Albania: somme case studies, Bull. Eng. Geol. Environ. 59 (2001) 313-318.

[2] T. Anovski, J. Naumovski, D. Kacurkov, P. Kirkov, A study of the origin of waters of St. Naum Springs, Lake Ohrid (in Macedonian), Fisica 12 (1980) 76–86.

[3] E. Bard, M. Arnold, B. Hamelin, N. Tisnerat-Laborde, G. Cabioch, Radiocarbon Calibration by Means of Mass Spectrometric $^{230}Th/^{234}U$ and ^{14}C Ages of Corals: An updated database including samples from Barbados, Mururoa, and Tahiti, In: Stuiver, M., and van der Plicht, J., eds. INTCAL98: Calibration Issue. Radiocarbon 40 (1998) 1085-1092.

[4] N. Calanchi, A. Cattaneo, E. Dinelli, G. Gasparotto, F. Lucchini, Tephra layers in Late Quaternary sediments of the central, Adriatic Sea. Marine Geology 149 (1998) 191–209.

[5] M. Coltelli, P. Del Carlo, L. Vezzoli, Stratigraphic constraints for explosive activity in the past 100 ka at Etna volcano, Italy, Int. J. Earth Sciences. 89 (2000) 665-677.

[6] B. De Vivo, G. Rolandi, P.B. Gans, A. Calvert, W.A. Bohrson, F.J. Spera, H.E. Belkin, News constraints on the pyroclastic eruptive history of the campagnian volcanic Plain (Italy), Mineralogy and Petrology. 73 (2001) 47-65.

[7] M.A. Di Vito, R. Sulpizio, G. Zanchetta, M. D'Orazio. The late Pleistocene pyroclastic deposits of the Campanian Plain: new insights into the explosive activity of Neapolitan volcanoes, J. Volcanol. Geotherm. Res. 177 (2008) 19-48 doi:10.1016/j.jvolgeores.2007.11.019.

[8] B. Giaccio, R. Isaia, F.G. Fedele, E. Di Canzio, J. Hoffecker, A. Ronchitelli, A. Sinitsyn, M. Anikovich, S.N. Lisitsyn, The Campanian Ignimbrite and Codola tephra layers: two temporal/stratigraphic markers for the Early Upper Palaeloithic in southern Italy and eastern Europe. J. Volcanol. Geotherm. Res. 177 (2008) 208-226 doi:10.1016/j.jvolgeores.2007.10.007.

[9] GSA Rock Color Chart (1991) The Geological Society of America Rock-Color Chart with genuine Munsell color chips. Printed by Munsell Color U.S.A.

[10] J. Keller, W.B.F. Ryan, D. Ninkovich, R. Altherr, Explosive volcanic activity in the Mediterranean over the past 200,000 yr as recorded in deep-sea sediments. Geol. Soc. Am. Bull. 89 (1978) 591–604.

[11] M. Kraml, Laser- 40Ar/39Ar-Datierungen an distalen marinen Tephren des jung-quartären mediterranen Vulkanismus (Ionishes Meer, METEOR-Fahrt 25/4), Ph.D. Thesis, Albert-Ludwigs-Universität Freiburg i.Br. (1997) 216 pp.

[12] M.J. Le Bas, R.W. Le Maitre, A. Streckeisen, B. Zanettin, A chemical classification of volcanic rocks based on the total alkali-silica diagram, J. Petrol. 27 (1986) 745–750.

[13] A.M. Lezine, U. von Grafenstein, N. Andersen, S. Belmecheri, A. Bordon, B. Caron, J.P. Cazet, H. Erlenkeuser, E. Fouache, C. Grenier, P. Huntsman-Mapila, D. Hureau-Mazaudier, D. Manelli, A. Mazaud, C. Robert, R. Sulpizio, J.J. Tiercelin, G. Zanchetta, Z. Zeqollari, Lake Ohrid, Albania, provides an exceptional multi-proxy record of environmental changes during the last glacial-interglacial cycle, PNAS (2009, submitted).

[14] J.J. Lowe, S. Blockley, F. Trincardi, A. Asioli, A. Cattaneo, I.P. Matthews, M. Pollard, S. Wulf, Age modelling of late Quaternary marine sequences in the Adriatic: towards improved precision and accuracy using volcanic event stratigraphy, Continental Shelf Research 27 (2007) 560–582.

[15] R. Macdonald,. Nomenclature and Petrochemistry of the Peralkaline Oversaturated Extrusive Rocks, Bull. Volcanol., 38 (1974) 498-516.

[16] M. Magny, J.L. de Beaulieu, R. Drescher-Schneider, B. Vannnière, A.V. Walter-Simmonet, L. Millet, G. Bossuet, O. Peyron, Climatic oscillations in central Italy during the Last Glacial-Holocene transition: the record from Lake Accesa, J. Quat. Sc. 21 (2006) 311-320.

[17] M. Magny, J.L. de Beaulieu, R. Drescher-Schneider, B. Vanniére, A.V. Walter- Simonnet, Y. Miras, L. Millet, G. Bossuet, O. Peyron, E. Brugiapaglia, A. Leroux, Holocene climate changes in the central Mediterranean as recorded by lake-level fluctuations at Lake Accesa (Tuscany, Italy), Quat. Sc. Rev. 26 (2007) 1736–1758.

[18] G.A. Mahood, W. Hildreth, Geology of the peralkaline volcano at Pantelleria, Strait of Sicily, Bull. Volcanol. 48 (1986) 143-172.

[19] P. Marianelli, A. Sbrana, Risultati di misure di standard di minerali e di vetri naturali in microanalisi a dispersione di energia, Atti Società Toscana di Scienze Naturali Memorie Serie A 105 (1998) 57-63.

[20] V. Margari, D.M. Pyle, C. Bryant, P.L. Gibbard, Mediterranean tephra stratigraphy revisited: Results from a long terrestrial sequence on Lesvos Island, Greece, J. Volcanol. Geotherm. Res. 163 (2007) 34-54.

[21] A. Matzinger, M. Jordanoski, E. Veljanoska-Sarafiloska, M. Sturm, B. Müller, A. Wüest, Is Lake Prespa jeopardizing the ecosystem of ancient Lake Ohrid? Hydrobiologica 553 (2006) 89–109.

[22] R. Munno, P. Petrosino, The late Quaternary tephrostratigraphical record of the San Gregorio Magno basin (southern Italy), J. Quat. Sc. 22 (2006) 247-266 doi:10.1002/jqs.1025.

[23] B.Narcisi, L. Vezzoli, Quaternary stratigraphy of distal tephra layers in the Mediterranean – an overview, Global and Planetary Change 21 (1999) 31-50.

[24] J. Nicot, M. Chardon, On the morphotectonic background and the evolution of natural environments and limestone relief in Western Yugoslavian Macedoni, Méditerranée (1983) 37-52

[25] L. Pappalardo, L. Civetta, M. D'Antonio, A. Deino, M.A. Di Vito, G. Orsi, A. Carandente, S. de Vita, R. Isaia, M. Piochi, Chemical and Sr-isotopical evolution of the Phlegraen magmatic system before the Campanian Ignimbrite and the Neapolitan Yellow Tuff eruptions, J. Volcanol. Geother. Res. 91 (1999) 141–166.

[26] M. Paterne, Reconstruction de l'activité explosive des volcans de l'Italie du Sud par tephrochronologie marine, Ph.D. Thesis University of Paris Sud XI, Paris (1985) 144 pp.

[27] M. Paterne, F.Guichard, J. Labeyrie, P.Y. Gillot, J.C. Duplessy, Tyrrhenian Sea tephrochronology of the oxygen isotope record for the past 60,000 years, Marine Geology, 72 (1986) 259-285.

[28] M. Paterne, F. Guichard, J. Labeyrie, Explosive activity of the South Italian volcanoes during the past 80,000 years as determined by marine tephrochronology, J. Volcanol. Geotherm. Res. 34, (1988) 153-172.

[29] M. Paterne, J. Labeyrie, F. Guichard, A. Massaud, F. Maitre, Fluctuation of the campanian explosive activity (South Italy) during the last 190,000 years as determined by marine tephrochronology, Earth and Planetary Science Letters 98 (1990) 166-174.

[30] M. Paterne, F. Guichard, J.C. Duplessy, G. Siani, R. Sulpizio, J. Labeyrie, A 90,000 – 200,000 yrs marine tephra record of Italian volcanic activity in the central Mediterranean Sea, J. Volcanol. Geotherm. Res. 177 (2008) 187-196 doi:10.1016/j.jvolgeores.2007.11.028.

[31] S. Poli, S. Chiesa, P.Y. Gillot, F. Guichard, Chemistry versus time in the volcanic complex of Ischia (Gulf of Naples, Italy): Evidence of successive magmatic cycles. Contrib. Min. Petrol. 95 (1987) 322-335.

[32] D.M. Pyle, G.D.Ricketts, V. Margari, T.H. van Andel, A.A. Sinitsyn, N. Praslov, S. Lisitsyn, Wide dispersal and deposition of distal tephra during the Pleistocene "Campanian Ignimbrite/Y5" eruption, Italy, Quat. Sc. Rev. 25 (2006) 2713–2728.

[33] P.J. Reimer, M.G.L.Baillie, E. Bard, A. Bayliss, J.W. Beck, C. Bertrand, P.G. Blackwell, C.E. Buck, G. Burr, K.B. Cutler, P.E. Damon, R.L. Edwards, R.G. Fairbanks, M. Friedrich, T.P. Guilderson, K.A. Hughen, B. Kromer, F.G. McCormac, S. Manning, C. Bronk Ramsey, R.W. Reimer, S. Remmele, J.R. Southon, M. Stuiver, S. Talamo, F.W. Taylor, J. van der Plicht, C.E. Weyhenmeyer, InterCal04 terrestrial radiocarbon age calibration, 0-26 kyrBP, Radiocarbon 46 (2004) 1029-1058.

[34] L. Sadori, B. Narcisi, The Postglacial record of environmental history from Lago di Pergusa, Sicily, The Holocene 11,6 (2001) 655-670. doi: 10.1191/09596830195681

[35] R. Santacroce, (Ed), Somma-Vesuvius, CNR Quaderni Ricerca Scientifica 114 (1987) 251.

[36] R. Santacroce, R. Cioni, P. Marianelli, A. Sbrana, R. Sulpizio, G. Zanchetta, D.J. Donahue, J.L. Joron, Age and whole rock-glass compositions of proximal pyroclastics from the major explosive eruptions of Somma-Vesuvius: a review as a tool for distal tephrostratigraphy, J. Volcanol. Geotherm. Res. 177 (2008) 1-18 doi:10.1016/j.jvolgeores.2008.06.009.

[37] G. Siani, R. Sulpizio, M. Paterne, A. Sbrana, Tephrostratigraphy study for the last 18,000 14C years in a deep-sea sediment sequence for the South Adriatic, Quat. Sc. Rev. 23 (2004) 2485-2500.

[38] S. Stankovic, The Balkan Lake Ohrid and its living world, Monographiae Biologicae IX, Dr. W. Junk, Den Haag, (1960) 357.

[39] R. Sulpizio, G. Zanchetta, M. Paterne, G. Siani, A review of tephrostratigraphy in central and southern Italy during the last 65 ka, Il Quaternario, 16 (2003) 91-108.

[40] R. Sulpizio, R. Bonasia, P. Dellino, M.A. Di Vito, L. La Volpe, D. Mele, G. Zanchetta, L. Sadori, Discriminating the long distance dispersal of fine ash from sustained columns or near ground ash clouds: the example of the Pomici di Avellino eruption (Somma-Vesuvius, Italy), J. Volcanol. Geotherm. Res. 177 (2008) 263-276 doi:10.1016/j.jvolgeores.2007.11.012.

[41] R. Sulpizio, A. van Welden, B. Caron, G. Zanchetta, The Holocene tephrostratigraphic record of Lake Shkodra (Albania and Montenegro), J. Quat. Sc. (2009, submitted).

[42] R. Thunnell, A. Federman, S. Sparks, D. Williams, The age, origin and volcanological significance of the Y-5 ash layer in the Mediterranean, Quaternary Research, 12 (1978) 241–253.

[43] P.C. Tzedakis, M.R.Frogley, T.H.E. Heaton, Last Interglacial conditions in southern Europe: evidence from Ioannina, northwest Greece, Global and Planetary Change 36 (2003) 157–170. doi:10.1016/S0921-8181(02)00182-0.

[44] L. Vezzoli, Island of Ischia. CNR, Quaderni della Ricerca Scientifica 114 (1988) 230.

[45] L. Vezzoli, Tephra layers in Bannock Basin (Eastern Mediterranean), Mar. Geol. 100 (1991) 21–34.

[46] B. Wagner, R. Sulpizio, G. Zanchetta, S. Wulf, M. Wessels, G. Daut, N. Nowaczyk, The last 40 ka tephrostratigraphic record of Lake Ohrid, Albania and Macedonia: a very distal archive for ash dispersal from Italian volcanoes, J. Volcanol. Geotherm. Res. 177 (2008) 71-80 doi:10.1016/j.jvolgeores.2007.08.018.

[47] S. Wulf, M. Kraml, A. Brauer, J. Keller, J.F.W. Negendank, Tephrochronology of the 100 ka lacustrine sediment record of Lago Grande di Monticchio (southern Italy), Quaternary International, 122 (2004) 7–30.

[48] S. Wulf, A. Brauer, J. Mingram, B. Zolitschka, J.F.W. Negendank, Distal tephras in the sediments of Monticchio maar lakes, In: C. Principe, Editor, La Geologia del Monte Vulture, Regione Basilicata – Consiglio Nazionale delle Ricerche, (2007) 105–122.

[49] G. Zanchetta, R. Sulpizio, B.Giaccio, G.Siani, M. Paterne, S. Wulf, M. D'Orazio, The Y-3 tephra: A Last Glacial stratigraphic marker for the central Mediterranean basin, J. Volcanol. Geotherm. Res. 177 (2008) 145-154 doi:10.1016/j.jvolgeores.2007.08.017.

Figure captions

Figure 1: Location map of the study area. The Italian volcanoes active in the investigated time span and the location of cores used in this study are also shown: CVZ = Campanian Volcanic Zone (Campi Flegrei, Somma-Vesuvius, Ischia and Procida), PRG = Lake of Pergusa, LGM = Lago Grande di Monticchio. In the framework in the upper right angle, the location of the JO 2004 core is shown.

Carte de localisation du site d'étude. Les principaux volcans Italiens actifs lors de la période étudiée et les sites des carottes utilisées dans cet article sont indiqués: CVZ = Campanian Volcanic Zone (Champs Phlégréens, Somma-Vesuvius, Ischia et Procida), PRG = lac de Pergusa, LGM = Lago Grande di Monticchio. En haut à droite, la position du site de forage de la carotte JO 2004.

Figure 2: Composite stratigraphy of the core JO 2004 (depth in cm): (a) lithostratigraphy (modified from [13]), (b) magnetic susceptibility curve and (c) relative glass shards abundance.

Stratigraphie recomposée de la carotte JO 2004 (profondeur en cm) : (a) lithostratigraphie (modifiée à partir de [13]), (b) courbe de susceptibilité magnétique et (c) abondance relative des esquilles de verres volcaniques.

Figure 3: Comparison of the compositions of the identified tephra layers and analyses from literature using the Total Alkali vs. Silica (TAS) diagram [12]. a) General classification using average glass analyses of the five identified tephra layers; b) plot of analyses of JO-941 cryptotephra and KET 8222-563 and 555 cm tephra from [30]; c) plot of analyses of JO-575 cryptotephra and KET 8222-350, 340 cm and DED 8708-1209 cm tephra from [26, 30]; d) plot of analyses of JO-244 tephra layer and TM-18 layer from [47] and ML-2 tephra layer from [20]; e) plot of analyses of JO-187 tephra layer and TM-15 tephra layer from [47] and MD90-917 920 cm tephra layer from [49] ; f) plot of analyses of JO-42 cryptotephra and SK13 514 cm and PRG06-03 390 cm from [41], Ohrid 310-315 cm tephra layer from [46] and Pergusa Type A and B from [34].

Comparaison entre les compositions chimiques des niveaux de tephra identifiés et ceux issus de la littérature dans un diagramme Total Alcalin vs. Silice (TAS) [12]. a) Diagramme général des moyennes des analyses sur les verres des cinq niveaux de tephra ; b) analyses du crytotephra JO-941 et des niveaux de tephra KET 8222-563 et 555 cm d'après [30]; c) analyses du crytotephra JO-575 et des niveaux de tephra KET 8222-350, 340 cm et DED 8708-1209 cm d'après [26, 30]; d) analyses du niveau de tephra JO-244 et des niveaux de tephra TM-18 d'après [47] et ML-2 d'après [20]; e) analyses du niveau de tephra JO-187 et des niveaux de tephra TM-15 d'après [47]

et MD 90-917 d'après [49]; f) analyses du crytotephra JO-42 et des niveaux de tephra de SK13 514 cm et PRG06-03 390 cm d'après [41], Ohrid 310-315 cm d'après [46] et Pergusa Type A et B d'après [34].

Figure 4: Scanning Electron Microscope (SEM) pictures of volcanic glass fragments from a) JO-941 sample, b) JO-575 sample, c) JO-244 sample, d) JO-187 sample and e) JO-42 sample.

Images au Microscope Electronique à Balayage (MEB) des échardes de verres volcaniques des niveaux a) JO-941, b) JO-575, c) JO-244, d) JO-187 et e) JO-42.

Figure 5: Dispersal areas of the five tephra layers recognized in core JO 2004. Y5 modified from [32] and [8] ; Etna FL modified from [41].

Cartes de dispersion des cinq éruptions identifiées dans la carotte JO 2004. Y5 est modifié à partir de [32] et [8] ; Etna FL est modifié à partir de [41].

Figure 6: Sedimentation curves for core JO 2004 calculated using the available calibrated ^{14}C (cross) and ages of tephra layers (diamonds). P11=JO-941, X6=JO-575, Y5=JO-245, Y3=JO-187, Etna FL=JO-42. Numbers in italic underlined indicate the calculated sedimentation rate (mm.yr^{-1}) for each segment of the curve.

Courbe de sédimentation de la carotte JO 2004 calculée à partir des âges ^{14}C calibrés (croix) et des datations des niveaux de tephra (losanges). P11=JO-941, X6=JO-575, Y5=JO-245, Y3=JO-187, Etna FL=JO-42. Les chiffres soulignés en italiques représentent le taux de sédimentation (mm.an^{-1}) pour chaque section de la courbe.

Table 1: Composition of major elements of the five tephra layers recognised in core JO 2004.

Compositions des éléments majeurs des cinq niveaux de tephra identifiés dans la carotte JO 2004.

Table 2: Comparison of average and standard deviation of analyses from literature used for comparison: KET 8222 340 cm, 350 cm, 555 cm, 563 cm, 765 cm, DED 8708 1209 cm from [26] and [30]; ML-2 from [20]; TM-15 and TM-18 from [47]; MD90-917 920cm from [49]; tephra Ohrid 310-315 cm from [46] ; Pergusa type A and B from [34] and PRG06-03 390 cm and SK13 514 cm from [41].

Comparaison des moyennes et des écarts types des analyses issues de la littérature: KET 8222 340 cm, 350 cm, 555 cm, 563 cm, 765 cm, DED 8708 1209 cm d'après [26] et [30]; ML-2 d'après [20]; TM-15 et TM-18 d'après [47]; MD90-917 920 cm d'après [49]; tephra Ohrid 310-315 cm d'après [46]; Pergusa type A et B d'après [34] et PRG06-03 390 cm et SK13 514 cm d'après [41].

Table 3: Conventional ^{14}C ages from JO 2004 core determined by UMS-ARTEMIS (Pelletron 3MV) AMS facilities (CNRS-CEA Saclay, France, [13]). Ages were calibrated using INTERCAL04 [33] for ^{14}C age younger than 26 cal ka BP and Bard polynomial equation for age older than 26 cal ka BP [3].

Tableau des âges AMS ^{14}C de la carotte JO 2004 obtenus par UMS-ARTEMIS (Pelletron 3MV) CNRS-CEA Saclay, France, [13]. Les âges ont été calibrés avec INTERCAL04 [33] pour les datations d'âge inférieur à 26 cal ka BP et avec le polynôme de Bard pour les datations d'âge supérieur à 26 cal ka [3].

Figure 1

Click here to download high resolution image

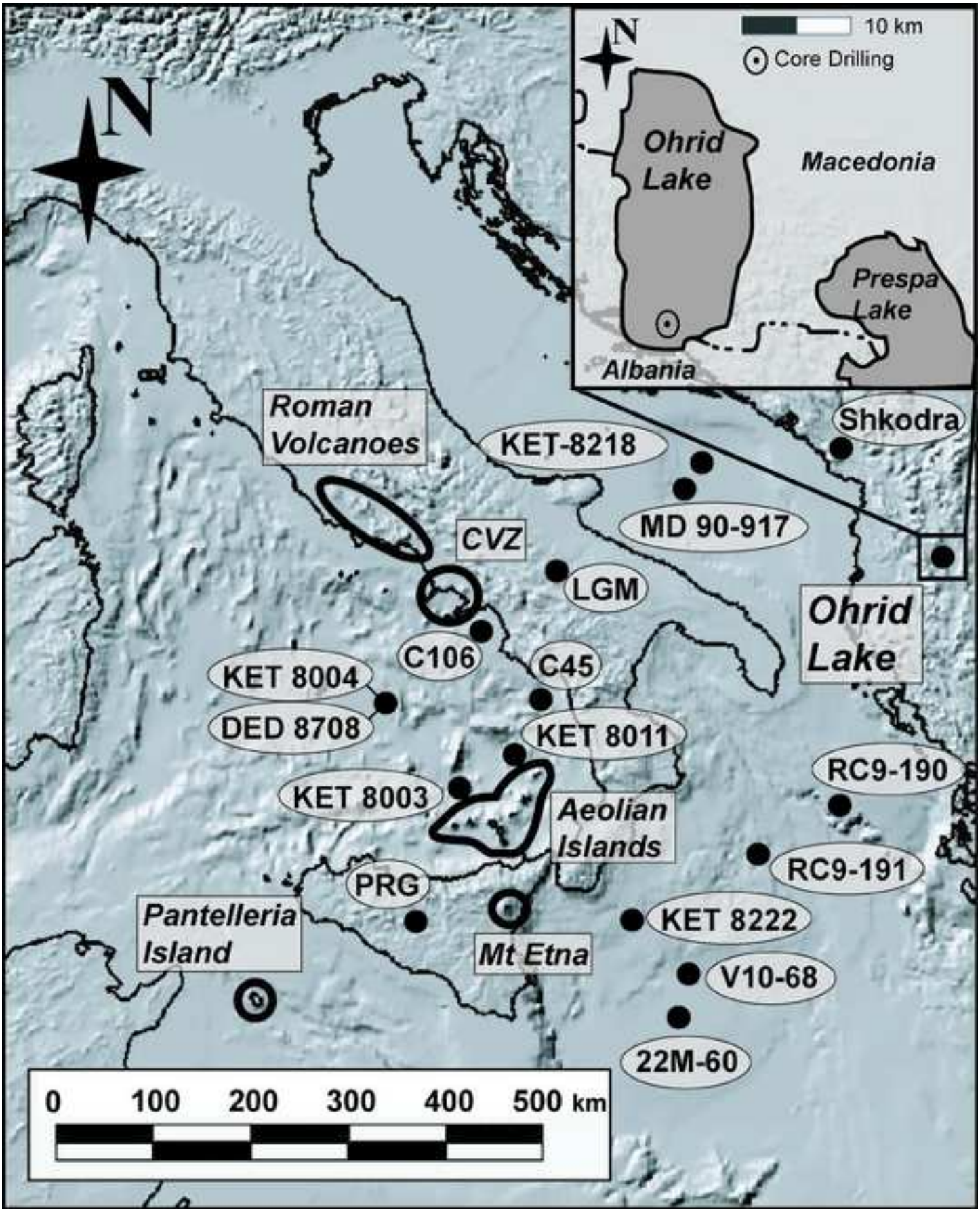

Figure 2

Click here to download high resolution image

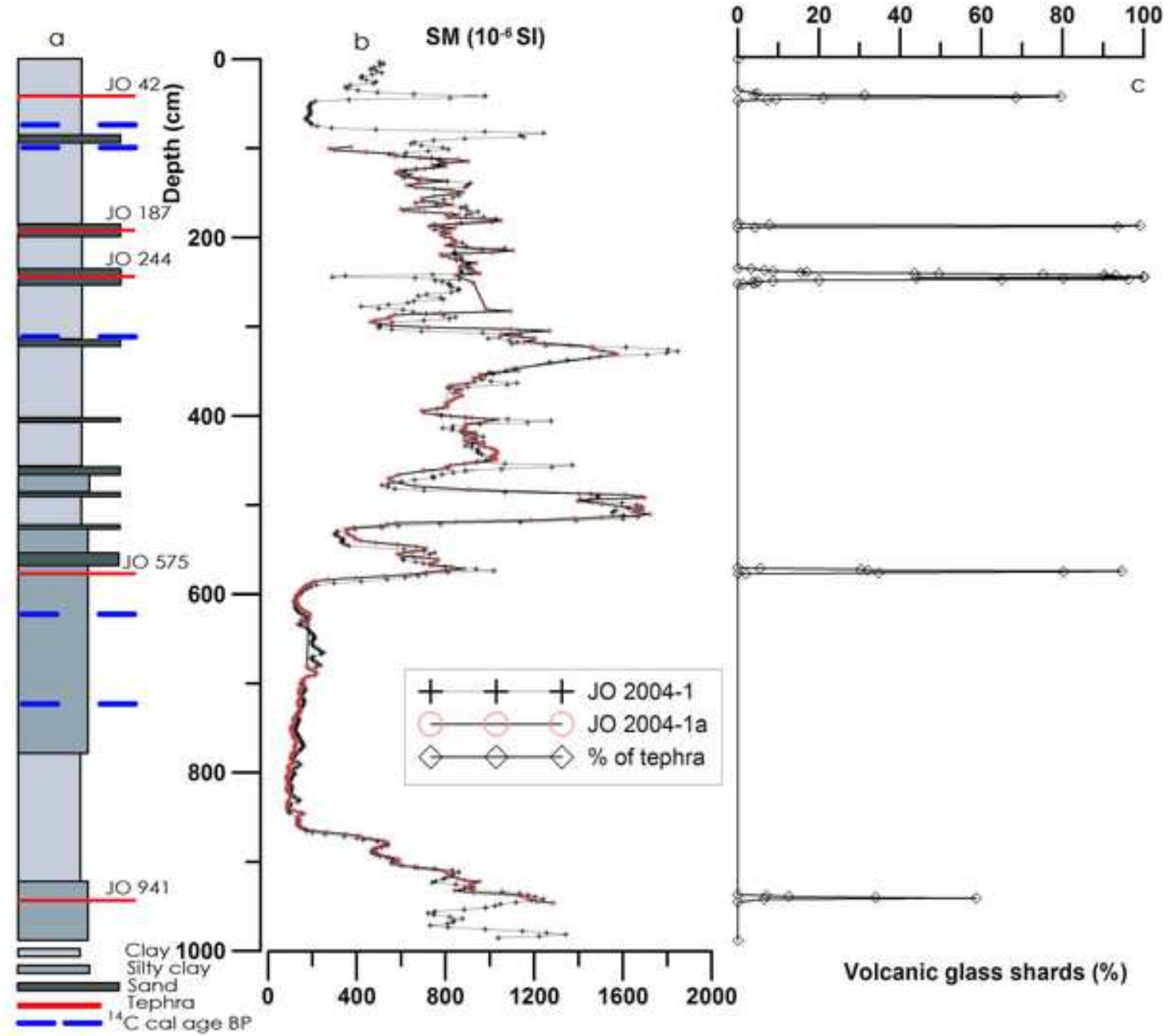

Figure 3

Click here to download high resolution image

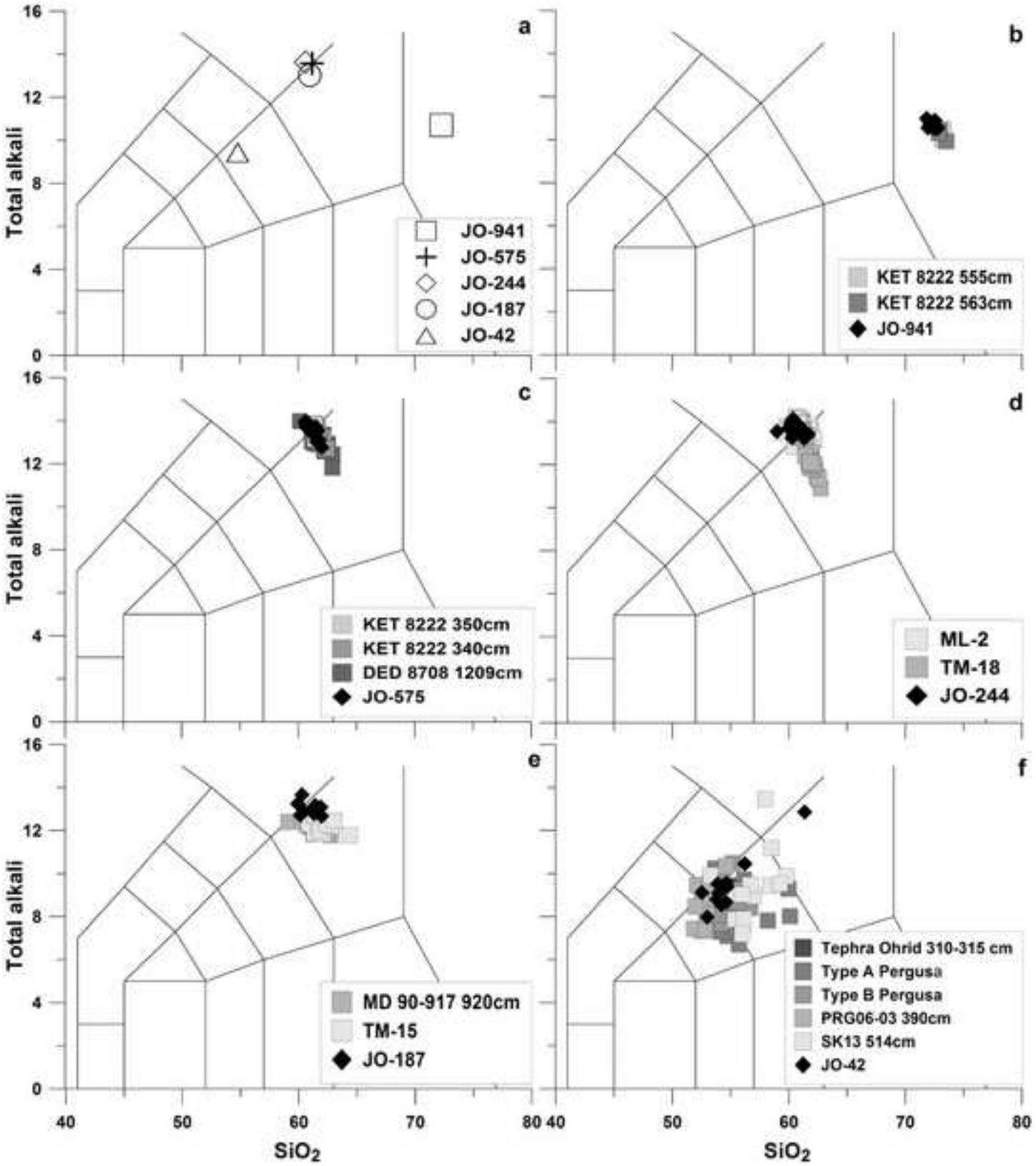

Figure 4

Click here to download high resolution image

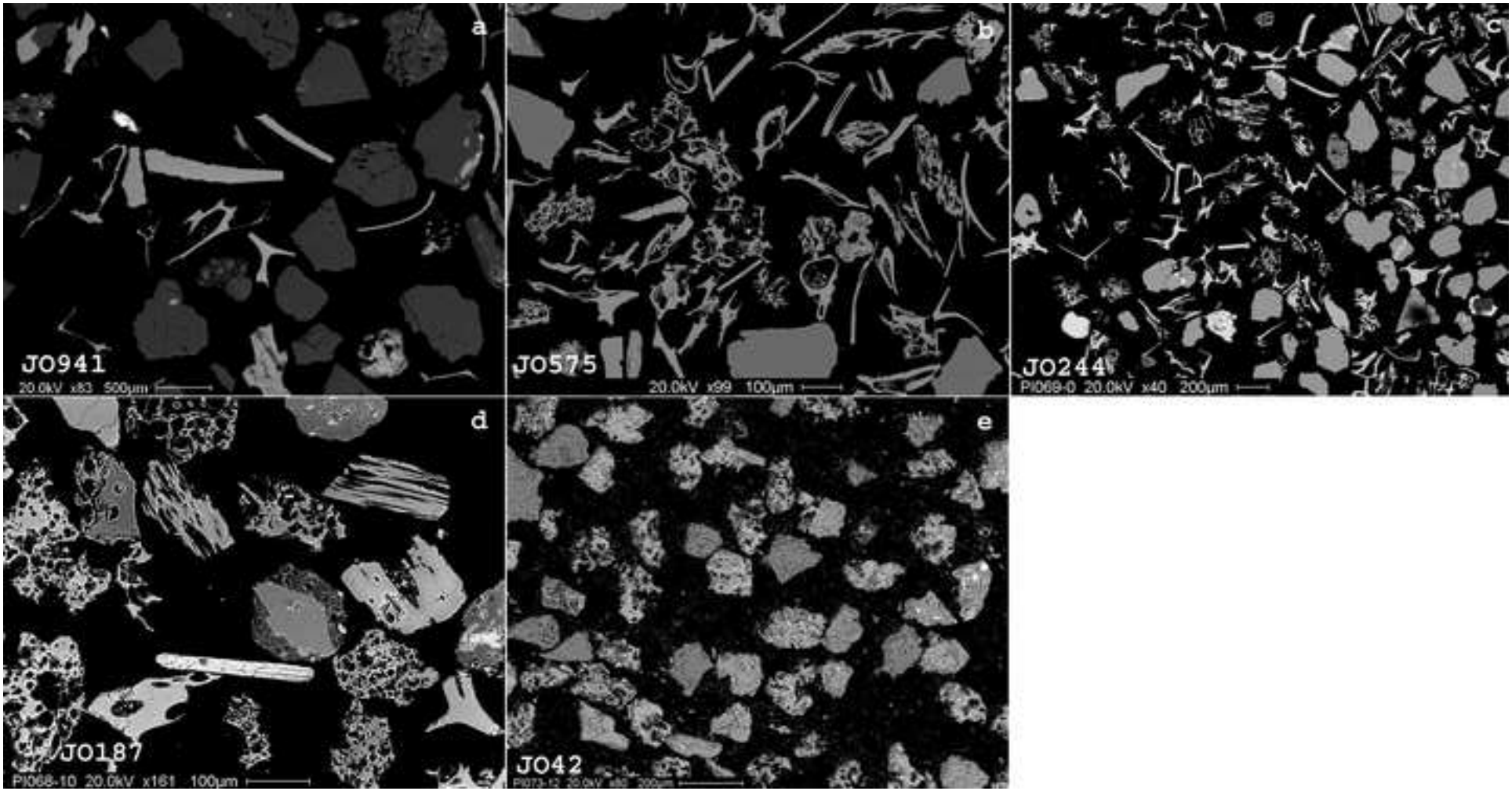

Figure 5

Click here to download high resolution image

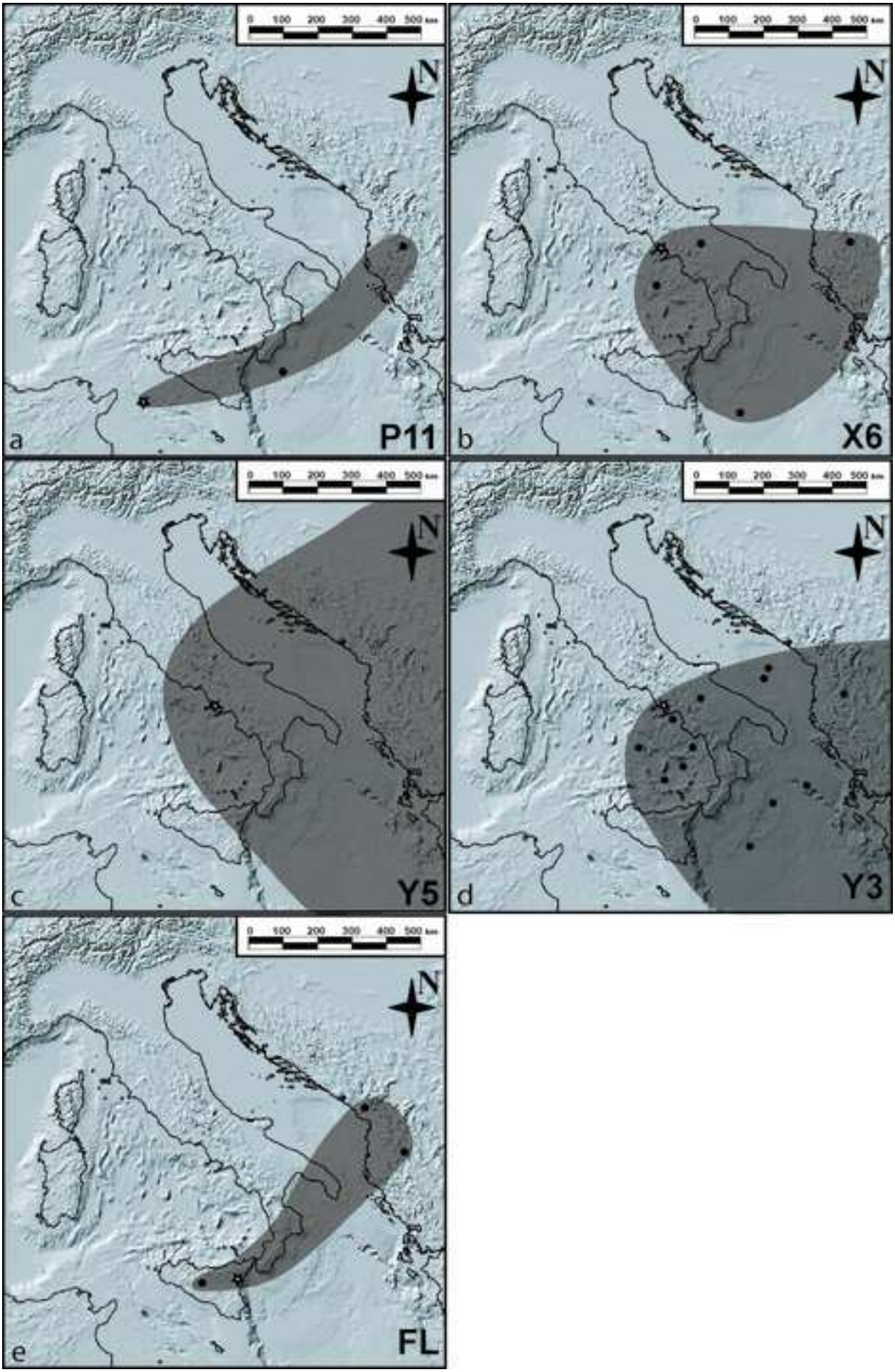

Figure 6

Click here to download high resolution image

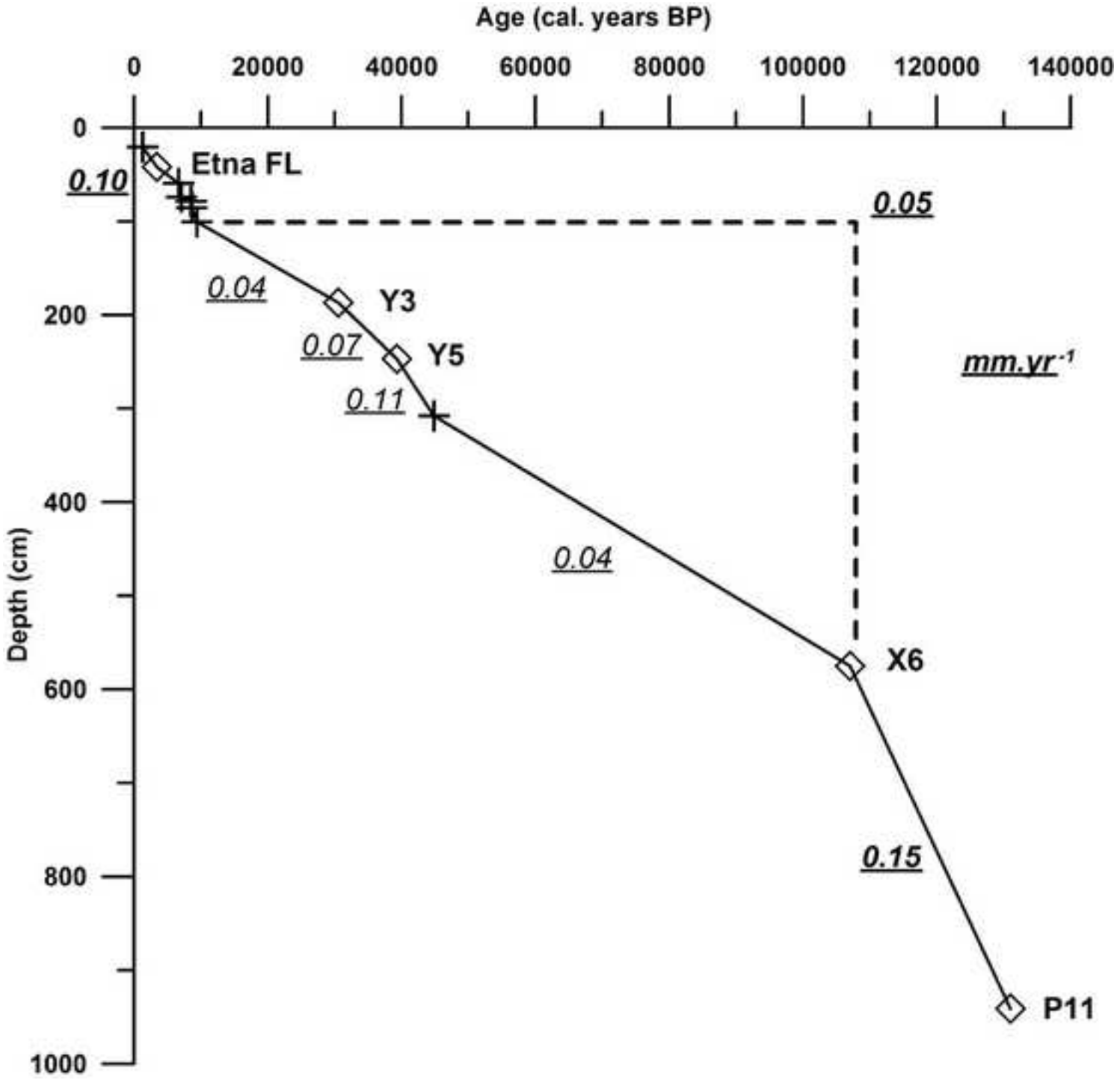

Table / Tableau 1

JO941	SiO_2	TiO_2	Al_2O_3	FeO_{tot}	MnO	MgO	CaO	Na_2O	K_2O
JO941-1	71.81	0.50	8.37	6.89	0.37	0.00	0.32	6.63	4.36
JO941-2	72.30	0.44	8.55	6.79	0.25	0.11	0.19	6.35	4.43
JO941-3	72.13	0.51	8.34	6.83	0.39	0.00	0.29	6.49	4.34
JO941-4	72.52	0.32	8.63	6.69	0.24	0.80	0.34	5.93	4.59
JO941-5	72.53	0.23	8.54	6.67	0.16	0.00	0.23	6.53	4.37
JO941-6	71.93	0.45	8.49	6.97	0.49	0.12	0.31	6.30	4.25
JO941-7	72.77	0.29	8.60	6.72	0.20	0.00	0.21	6.16	4.37
JO941-8	72.30	0.35	8.62	6.83	0.23	0.08	0.22	6.41	4.29
JO941-9	72.07	0.27	8.61	6.91	0.23	0.10	0.32	6.44	4.37
JO941-10	72.24	0.32	8.53	6.85	0.38	0.00	0.32	6.18	4.42
JO941-11	72.30	0.45	8.54	6.64	0.26	0.10	0.36	6.21	4.50
JO941-12	72.61	0.17	8.68	6.63	0.18	0.00	0.34	6.33	4.32
JO941-13	72.11	0.49	8.57	6.81	0.34	0.04	0.26	6.28	4.42
Mean	**72.28**	**0.37**	**8.54**	**6.79**	**0.29**	**0.10**	**0.29**	**6.33**	**4.39**
Sd	*0.28*	*0.11*	*0.10*	*0.11*	*0.10*	*0.21*	*0.06*	*0.18*	*0.09*

JO575	SiO_2	TiO_2	Al_2O_3	FeO_{tot}	MnO	MgO	CaO	Na_2O	K_2O
JO575-1	60.59	0.53	18.42	3.24	0.39	0.27	1.78	7.29	6.66
JO575-2	61.01	0.59	18.86	2.85	0.31	0.38	1.54	6.82	6.93
JO575-3	60.90	0.44	18.46	3.13	0.20	0.31	1.84	7.08	6.76
JO575-4	60.90	0.46	18.84	2.93	0.21	0.26	1.68	7.28	6.57
JO575-5	60.71	0.50	18.63	3.08	0.40	0.47	1.63	6.85	6.94
JO575-6	61.69	0.50	18.53	2.78	0.23	0.46	1.69	5.80	7.74
JO575-7	61.48	0.36	18.74	2.80	0.13	0.36	1.84	5.62	8.11
JO575-8	61.16	0.46	18.69	3.00	0.30	0.30	1.65	6.86	6.85
JO575-9	60.69	0.61	18.54	3.21	0.40	0.39	1.59	7.20	6.56
JO575-10	61.67	0.43	18.64	2.93	0.30	0.50	1.59	6.02	7.49
JO575-11	61.68	0.64	18.79	2.82	0.42	0.35	1.50	6.33	6.81
JO575-12	61.13	0.50	18.90	3.10	0.38	0.30	1.51	6.70	6.73
JO575-13	61.83	0.52	18.69	2.95	0.27	0.43	1.56	5.56	7.54
JO575-14	61.58	0.49	19.07	2.69	0.28	0.52	1.76	5.53	7.49
JO575-15	61.11	0.37	18.85	3.00	0.24	0.43	1.59	6.73	6.87
JO575-16	60.65	0.46	18.74	3.13	0.36	0.30	1.70	7.22	6.58
JO575-17	60.73	0.35	18.92	3.02	0.34	0.35	1.73	7.08	6.60
JO575-18	61.43	0.36	18.66	2.87	0.20	0.46	1.74	6.00	7.70
JO575-19	62.04	0.38	18.96	2.86	0.24	0.42	1.61	5.87	6.89
JO575-20	60.92	0.41	18.87	3.09	0.20	0.38	1.45	6.96	6.89
Mean	**61.20**	**0.47**	**18.74**	**2.97**	**0.29**	**0.38**	**1.65**	**6.54**	**7.04**
Sd	*0.45*	*0.08*	*0.17*	*0.15*	*0.08*	*0.08*	*0.11*	*0.63*	*0.46*

JO244	SiO_2	TiO_2	Al_2O_3	FeO_{tot}	MnO	MgO	CaO	Na_2O	K_2O
JO244-1	60.87	0.46	19.19	2.97	0.20	0.38	1.59	6.62	7.08
JO244-2	61.16	0.33	19.08	2.93	0.20	0.34	1.81	5.98	7.49
JO244-3	60.68	0.42	19.04	2.94	0.21	0.38	1.88	6.25	7.51
JO244-4	60.60	0.52	19.17	2.85	0.25	0.35	1.69	6.53	7.24
JO244-5	60.57	0.51	19.11	2.90	0.31	0.51	1.68	6.58	7.17
JO244-6	59.96	0.36	19.47	3.14	0.23	0.40	1.92	6.10	7.60
JO244-7	61.00	0.38	19.10	2.86	0.18	0.28	1.78	6.48	7.22

JO244-8	60.62	0.55	19.09	2.99	0.26	0.47	1.75	6.37	7.31
JO244-9	60.34	0.37	19.84	2.97	0.20	0.40	1.73	6.21	7.28
JO244-10	61.67	0.44	19.08	2.65	0.15	0.36	1.68	6.07	7.34
JO244-11	58.97	0.45	19.68	3.48	0.07	0.80	2.60	5.08	8.46
JO244-12	60.93	0.36	19.00	2.99	0.21	0.22	1.73	6.42	7.35
JO244-13	60.86	0.45	19.08	2.87	0.21	0.32	1.70	6.37	7.39
JO244-14	60.78	0.45	18.97	2.93	0.19	0.42	1.80	6.33	7.39
JO244-15	61.31	0.26	19.25	2.92	0.19	0.34	1.80	5.65	7.57
JO244-16	60.16	0.49	19.13	2.98	0.28	0.42	1.87	6.13	7.84
JO244-18	60.76	0.29	18.94	2.96	0.28	0.37	1.83	6.39	7.49
JO244-19	60.35	0.46	18.97	2.97	0.20	0.40	1.72	6.31	7.82
Mean	**60.64**	**0.42**	**19.18**	**2.96**	**0.21**	**0.40**	**1.81**	**6.22**	**7.48**
Sd	*0.58*	*0.08*	*0.25*	*0.16*	*0.05*	*0.12*	*0.21*	*0.37*	*0.32*

JO244-17	60.26	0.38	18.80	3.33	0.07	0.96	2.66	3.34	9.92
JO244-20	60.38	0.28	19.14	3.24	0.00	0.69	2.60	3.15	10.22
Mean	**60.32**	**0.33**	**18.97**	**3.29**	**0.04**	**0.83**	**2.63**	**3.25**	**10.07**
Sd	*0.08*	*0.07*	*0.24*	*0.06*	*0.05*	*0.19*	*0.04*	*0.13*	*0.21*

JO188	**SiO_2**	**TiO_2**	**Al_2O_3**	**FeO_{tot}**	**MnO**	**MgO**	**CaO**	**Na_2O**	**K_2O**
JO188-1	61.22	0.42	18.77	3.18	0.11	0.67	2.26	3.62	9.39
JO188-2	60.43	0.52	18.89	3.40	0.09	0.77	2.63	3.44	9.48
JO188-3	60.11	0.49	18.71	3.74	0.12	0.93	2.87	3.13	9.59
JO188-4	61.30	0.33	18.70	3.31	0.06	0.69	2.49	2.96	9.82
JO188-5	60.25	0.50	18.85	3.27	0.28	0.64	2.03	4.32	9.35
JO188-6	61.88	0.31	18.53	2.90	0.12	0.47	2.22	3.83	9.26
JO188-7	59.89	0.53	18.75	3.64	0.10	0.87	2.63	2.95	10.30
JO188-8	61.40	0.35	18.68	3.07	0.17	0.42	2.16	4.38	8.79
JO188-9	61.47	0.32	18.70	3.09	0.00	0.72	2.32	3.53	9.42
JO188-10	61.94	0.26	18.81	2.98	0.06	0.64	2.19	3.77	8.90
Mean	**60.99**	**0.40**	**18.74**	**3.26**	**0.11**	**0.68**	**2.38**	**3.59**	**9.43**
Sd	*0.75*	*0.10*	*0.10*	*0.27*	*0.07*	*0.16*	*0.26*	*0.50*	*0.43*

JO42	**SiO_2**	**TiO_2**	**Al_2O_3**	**FeO_{tot}**	**MnO**	**MgO**	**CaO**	**Na_2O**	**K_2O**
JO42-1	52.98	1.79	17.85	8.38	0.25	3.27	6.79	5.30	2.68
JO42-2	54.60	1.63	18.10	7.39	0.22	2.39	6.14	5.65	3.03
JO42-3	53.79	1.67	17.76	8.52	0.00	2.72	5.90	5.57	3.23
JO42-4	54.69	1.86	18.00	7.45	0.28	2.03	5.45	5.72	3.67
JO42-5	53.96	1.70	17.41	7.92	0.14	2.99	6.05	5.94	3.15
JO42-7	52.51	2.23	16.55	9.77	0.25	2.84	5.86	5.18	3.94
JO42-8	53.88	1.83	17.81	8.41	0.09	2.57	5.24	5.97	3.56
JO42-9	61.35	0.53	18.75	3.06	0.24	0.54	2.18	3.96	8.90
JO42-11	54.20	1.84	17.05	8.13	0.24	2.98	6.23	5.23	3.32
JO42-12	56.22	1.50	19.13	5.45	0.09	1.12	5.24	6.53	3.93
JO42-13	54.61	1.86	17.53	7.68	0.18	2.38	5.28	5.67	3.89
Mean	**54.80**	**1.68**	**17.81**	**7.47**	**0.18**	**2.35**	**5.49**	**5.52**	**3.94**
Sd	*2.38*	*0.42*	*0.72*	*1.80*	*0.09*	*0.83*	*1.20*	*0.65*	*1.70*

P_2O_5	ClO	Total	Total Alkali
0.00	0.76	100.01	10.99
0.00	0.61	100.02	10.78
0.00	0.68	100.00	10.83
0.00	0.66	100.72	10.52
0.00	0.75	100.01	10.90
0.00	0.69	100.00	10.55
0.00	0.67	99.99	10.53
0.00	0.67	100.00	10.70
0.00	0.68	100.00	10.81
0.00	0.76	100.00	10.60
0.00	0.64	100.00	10.71
0.00	0.74	100.00	10.65
0.00	0.68	100.00	10.70
0.00	**0.69**	-	**10.71**
0.00	*0.05*	-	-

P_2O_5	ClO	Total	Total Alkali
0.00	0.82	99.99	13.95
0.00	0.71	100.00	13.75
0.00	0.87	99.99	13.84
0.00	0.88	100.01	13.85
0.00	0.78	99.99	13.79
0.00	0.57	99.99	13.54
0.00	0.57	100.01	13.73
0.00	0.73	100.00	13.71
0.00	0.81	100.00	13.76
0.00	0.44	100.01	13.51
0.00	0.65	99.99	13.14
0.00	0.75	100.00	13.43
0.00	0.64	99.99	13.10
0.00	0.59	100.00	13.02
0.00	0.80	99.99	13.60
0.00	0.85	99.99	13.80
0.00	0.88	100.00	13.68
0.00	0.57	99.99	13.70
0.00	0.73	100.00	12.76
0.00	0.82	99.99	13.85
0.00	**0.72**	-	**13.58**
0.00	*0.13*	-	-

P_2O_5	ClO	Total	Total Alkali
0.00	0.65	100.01	13.70
0.00	0.68	100.00	13.47
0.00	0.68	99.99	13.76
0.00	0.80	100.00	13.77
0.00	0.65	99.99	13.75
0.00	0.82	100.00	13.70
0.00	0.71	99.99	13.70

0.00	0.61	100.02	13.68
0.00	0.66	100.00	13.49
0.00	0.58	100.02	13.41
0.00	0.41	100.00	13.54
0.00	0.79	100.00	13.77
0.00	0.75	100.00	13.76
0.00	0.75	100.01	13.72
0.00	0.71	100.00	13.22
0.00	0.71	100.01	13.97
0.00	0.70	100.01	13.88
0.00	0.81	100.01	14.13
0.00	**0.69**	-	**13.69**
0.00	*0.10*	-	-

0.00	0.30	100.02	13.26
0.00	0.30	100.00	13.37
0.00	**0.30**	-	**13.66**
0.00	*0.00*	-	-

P_2O_5	ClO	Total	Total Alkali
0.00	0.36	100.00	13.01
0.00	0.35	100.00	12.92
0.00	0.31	100.00	12.72
0.00	0.33	99.99	12.78
0.00	0.51	100.00	13.67
0.00	0.49	100.01	13.09
0.00	0.35	100.01	13.25
0.00	0.59	100.01	13.17
0.00	0.44	100.01	12.95
0.00	0.44	99.99	12.67
0.00	**0.42**	-	**13.02**
0.00	*0.09*	-	-

P_2O_5	ClO	Total	Total Alkali
0.38	0.33	100.00	7.98
0.51	0.31	99.97	8.68
0.51	0.32	99.99	8.80
0.54	0.30	99.99	9.39
0.44	0.31	100.01	9.09
0.54	0.33	100.00	9.12
0.38	0.26	100.00	9.53
0.00	0.49	100.00	12.86
0.51	0.27	100.00	8.55
0.44	0.34	99.99	10.46
0.57	0.35	100.00	9.56
0.44	**0.33**	-	**9.46**
0.16	*0.06*	-	-

Table / Tableau 2

		SiO_2	TiO_2	Al_2O_3	FeO_{tot}	MnO	MgO	CaO	Na_2O	K_2O	P_2O_5
KET 8222 563cm	**mean**	**73.09**	**0.39**	**8.88**	**7.05**	**-**	**0.09**	**0.27**	**5.81**	**4.42**	**-**
n=13	*sd*	*0.36*	*0.08*	*0.13*	*0.12*	*-*	*0.06*	*0.11*	*0.37*	*0.16*	*-*
KET 8222 555cm	**mean**	**72.95**	**0.31**	**8.89**	**7.23**	**-**	**0.05**	**0.20**	**5.90**	**4.48**	**-**
n=13	*sd*	*0.47*	*0.05*	*0.05*	*0.33*	*-*	*0.03*	*0.04*	*0.36*	*0.10*	*-*
KET 8222 765cm	**mean**	**72.97**	**0.50**	**9.02**	**7.34**	**-**	**0.10**	**0.20**	**5.44**	**4.42**	**-**
	sd	*0.49*	*0.06*	*0.16*	*0.28*	*-*	*0.07*	*0.02*	*0.30*	*0.06*	*-*

		SiO_2	TiO_2	Al_2O_3	FeO_{tot}	MnO	MgO	CaO	Na_2O	K_2O	P_2O_5
KET8222 350cm	**mean**	**61.47**	**0.52**	**19.20**	**3.20**	**-**	**0.40**	**1.66**	**6.27**	**7.30**	**-**
n=11	*sd*	*0.06*	*0.04*	*0.10*	*0.22*	*-*	*0.06*	*0.10*	*0.53*	*0.77*	*-*
KET8222 340cm	**mean**	**61.98**	**0.47**	**19.18**	**3.06**	**-**	**0.42**	**1.70**	**6.08**	**7.11**	**-**
n=14	*sd*	*0.27*	*0.10*	*0.13*	*0.15*	*-*	*0.09*	*0.10*	*0.68*	*0.46*	*-*
DED 8708 1209cm	**mean**	**61.81**	**0.48**	**18.18**	**3.04**	**0.33**	**0.31**	**1.71**	**5.72**	**7.29**	**0.02**
n=19	*sd*	*0.68*	*0.10*	*0.31*	*0.23*	*0.12*	*0.07*	*0.32*	*0.91*	*0.86*	*0.04*

		SiO_2	TiO_2	Al_2O_3	FeO_{tot}	MnO	MgO	CaO	Na_2O	K_2O	P_2O_5
TM-18	**mean**	**61.69**	**0.42**	**19.11**	**2.93**	**0.24**	**0.35**	**1.73**	**5.66**	**6.83**	**0.05**
n=43	*sd*	*0.46*	*0.02*	*0.21*	*0.09*	*0.02*	*0.02*	*0.07*	*0.71*	*0.29*	*0.03*
ML-2	**mean**	**61.01**	**0.48**	**18.18**	**3.02**	**0.21**	**0.44**	**2.12**	**5.64**	**8.05**	**0.07**
n=105	*sd*	*0.42*	*0.04*	*0.19*	*0.21*	*0.06*	*0.15*	*0.32*	*1.21*	*1.02*	*0.04*

		SiO_2	TiO_2	Al_2O_3	FeO_{tot}	MnO	MgO	CaO	Na_2O	K_2O	P_2O_5
TM-15	**mean**	**62.22**	**0.38**	**18.36**	**3.27**	**0.13**	**0.61**	**2.19**	**3.85**	**8.36**	**0.12**
n=20	*sd*	*0.78*	*0.03*	*0.21*	*0.29*	*0.04*	*0.15*	*0.22*	*0.44*	*0.55*	*0.06*
MD90-917 920cm	**mean**	**61.41**	**0.36**	**18.72**	**3.17**	**0.08**	**0.70**	**2.44**	**3.52**	**9.14**	**-**
n=20	*sd*	*0.86*	*0.12*	*0.17*	*0.38*	*0.08*	*0.21*	*0.33*	*0.40*	*0.40*	*-*

		SiO_2	TiO_2	Al_2O_3	FeO_{tot}	MnO	MgO	CaO	Na_2O	K_2O	P_2O_5
SK13 514cm	**mean**	**56.81**	**1.21**	**20.52**	**4.86**	**0.09**	**1.38**	**5.27**	**6.22**	**3.10**	**0.24**
n=14	*sd*	*1.78*	*0.44*	*2.39*	*2.49*	*0.09*	*1.27*	*1.83*	*1.04*	*1.26*	*0.22*
Tephra Ohrid 310-315 cm	**mean**	**54.25**	**1.76**	**17.48**	**8.15**	**0.00**	**2.85**	**6.02**	**5.40**	**3.29**	**0.48**
n=15	*sd*	*0.73*	*0.22*	*0.51*	*0.53*	*0.00*	*0.33*	*0.50*	*0.41*	*0.34*	*0.10*
PRG06-03 390 cm	**mean**	**52.82**	**2.04**	**16.86**	**9.43**	**0.23**	**3.21**	**6.13**	**4.99**	**3.58**	**0.47**
n=11	*sd*	*0.82*	*0.17*	*0.47*	*0.90*	*0.10*	*0.42*	*1.03*	*0.37*	*0.67*	*0.07*
Type A Pergusa	**mean**	**55.61**	**1.58**	**16.97**	**7.25**	**0.15**	**3.98**	**5.62**	**6.02**	**2.37**	**-**
n=14	**sd**	*2.28*	*0.20*	*0.78*	*1.35*	*0.09*	*0.57*	*0.95*	*1.13*	*0.34*	*-*
Type B Pergusa	**mean**	**54.91**	**1.61**	**17.65**	**6.83**	**0.15**	**3.90**	**5.65**	**5.79**	**3.06**	**-**
n=11	**sd**	*0.91*	*0.23*	*0.49*	*1.16*	*0.09*	*0.47*	*1.04*	*0.88*	*0.25*	*-*

SO_3	ClO	F	Total Alkali
-	**-**	**-**	**10.23**
-	-	-	-
-	**-**	**-**	**10.38**
-	-	-	-
-	**-**	**-**	**9.86**
-	-	-	-

SO_3	ClO	F	Total Alkali
-	**-**	**-**	**13.56**
-	-	-	-
-	**-**	**-**	**13.19**
-	-	-	-
0.11	**0.97**	**-**	**13.02**
0.08	*0.28*	-	-

SO_3	ClO	F	Total Alkali
-	**0.78**	**0.19**	**12.49**
-	*0.05*	*0.17*	-
-	**0.71**	**-**	**13.70**
-	*0.20*	-	-

SO_3	ClO	F	Total Alkali
-	**0.52**	**0.00**	**12.21**
-	*0.11*	*0.00*	-
-	**0.44**	**-**	**12.66**
-	*0.09*	-	-

SO_3	ClO	F	Total Alkali
-	**0.30**	**-**	**9.32**
-	*0.11*	-	-
-	**0.31**	**-**	**8.69**
-	*0.06*	-	-
-	**0.24**	**-**	**8.57**
-	*0.06*	-	-
-	**0.46**	**-**	**8.39**
-	*0.09*	-	-
-	**0.45**	**-**	**8.86**
-	*0.43*	-	-

Table / Tableau 3

Laboratory number (Artemis-Saclay)	Sample	Mean composite Depth (cm)	^{14}C age	error	age cal final	erreur 1 s	Methods
SacA 8010	JO2004-1A020	20.5	1285	30	1253	30	intcal04 Reimer et al., 2004
SacA 8011	JO2004-1A059	59.5	5840	35	6680	66	intcal04 Reimer et al., 2004
2653	JO2004-1A074	74	6130	80	7048	156	intcal04 Reimer et al., 2004
2654	JO2004-1A078	78.5	7800	80	8550	139	intcal04 Reimer et al., 2004
SacA 8012	JO2004-1A085	85.5	7850	40	8622	52	intcal04 Reimer et al., 2004
SacA 8013	JO2004-1A100	100.5	8275	40	9407	121	intcal04 Reimer et al., 2004
2655	JO2004-1B113	307.6	39100	1200	44812	1055	Bard et al., 1998